Discovery of 4-Aryl-5,6,7,8-tetrahydroisoquinolines as Potent, Selective, and Orally Active Aldosterone Synthase (CYP11B2) Inhibitors: In Vivo Evaluation in Rodents and Cynomolgus Monkeys

Rainer E. Martin,[†] Johannes D. Aebi,*,[†] Benoit Hornsperger,[†] Hans-Jakob Krebs,[†] Bernd Kuhn,[†] Andreas Kuglstatter,[†] André M. Alker,[†] Hans Peter Märki,[†] Stephan Müller,[‡] Dominique Burger,[‡] Giorgio Ottaviani,[§] William Riboulet,[∥] Philippe Verry,[⊥] Xuefei Tan,[#] Kurt Amrein,*,[∇] and Alexander V. Mayweg*,[†]

[†]Medicinal Chemistry, Roche Pharma Research and Early Development (pRED), Roche Innovation Center Basel, F. Hoffmann-La Roche Ltd., Grenzacherstrasse 124, CH-4070 Basel, Switzerland

[‡]Discovery Technologies, Roche Pharma Research and Early Development (pRED), Roche Innovation Center Basel, F. Hoffmann-La Roche Ltd., Grenzacherstrasse 124, CH-4070 Basel, Switzerland

[§]Pharmaceutical Sciences, Roche Pharma Research and Early Development (pRED), Roche Innovation Center Shanghai, F. Hoffmann-La Roche Ltd., 720 Cai Lun Road, Building 5, Pudong, Shanghai 201203, China

[∥]Neuroscience, Ophthalmology and Rare Diseases, Roche Pharma Research and Early Development (pRED), Roche Innovation Center Basel, F. Hoffmann-La Roche Ltd., Grenzacherstrasse 124, CH-4070 Basel, Switzerland

[⊥]Discovery Cardiovascular and Metabolic Disease, Roche Pharma Research and Early Development (pRED), Roche Innovation Center Basel, F. Hoffmann-La Roche Ltd., Grenzacherstrasse 124, CH-4070 Basel, Switzerland

[#]Medicinal Chemistry, Roche Pharma Research and Early Development (pRED), Roche Innovation Center Shanghai, F. Hoffmann-La Roche Ltd., 720 Cai Lun Road, Building 5, Pudong, Shanghai 201203, China

[∇]Discovery Infectious Disease, Roche Pharma Research and Early Development (pRED), Roche Innovation Center Basel, F. Hoffmann-La Roche Ltd., Grenzacherstrasse 124, CH-4070 Basel, Switzerland

S *Supporting Information*

ABSTRACT: Inappropriately high levels of aldosterone are associated with many serious medical conditions, including renal and cardiac failure. A focused screen hit has been optimized into a potent and selective aldosterone synthase (CYP11B2) inhibitor with in vitro activity against rat, mouse, human, and cynomolgus monkey enzymes, showing a selectivity factor of 160 against cytochrome CYP11B1 in the

last species. The novel tetrahydroisoquinoline compound (+)-(R)-6 selectively reduced aldosterone plasma levels in vivo in a dose-dependent manner in db/db mice and cynomolgus monkeys. The selectivity against CYP11B1 as predicted by cellular inhibition data and free plasma fraction translated well to Synacthen challenged cynomolgus monkeys up to a dose of 0.1 mg kg^{-1}. This compound, displaying good in vivo potency and selectivity in mice and monkeys, is ideally suited to perform mechanistic studies in relevant rodent models and to provide the information necessary for translation to non-human primates and ultimately to man.
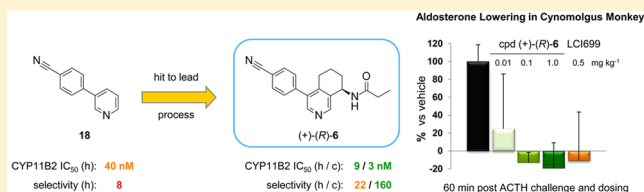
INTRODUCTION

The renin angiotensin aldosterone system (RAAS) is a pathway that has been linked to hypertension, volume, and salt balance and more recently to contribute directly to end organ damage in advanced stages of heart failure or kidney disease.[1] Beyond blood pressure control the RAAS plays an important role in the pathogenesis of a variety of clinical conditions such as atherosclerosis, left ventricular hypertrophy, myocardial infarction, and heart failure.[1] In particular it has been demonstrated that activation of RAAS is associated with an increased risk of ischemic cardiovascular events independent from blood pressure.[2] Moreover blocking the RAAS can

provide protection against renal injury in patients with chronic kidney disease (CKD).[3]

Angiotensin-converting enzyme (ACE) inhibitors and angiotensin receptor blockers (ARBs) are successfully used to improve duration and quality of life of patients. However, although indispensable from today's treatment regiment, these drugs do not yield maximum protection. In a relatively large number of patients these drugs lead to so-called aldosterone breakthrough, a phenomenon where aldosterone levels, after a

Fadrozole (FAD286), 1

CYP11B2 IC$_{50}$ (h):   6 nM

CYP11B2 IC$_{50}$ (m): 190 nM

selectivity factor (h):   12

LCI699 (Novartis, Phase II), 2

CYP11B2 IC$_{50}$ (h):   3 nM

CYP11B2 IC$_{50}$ (m): 210 nM

6

3

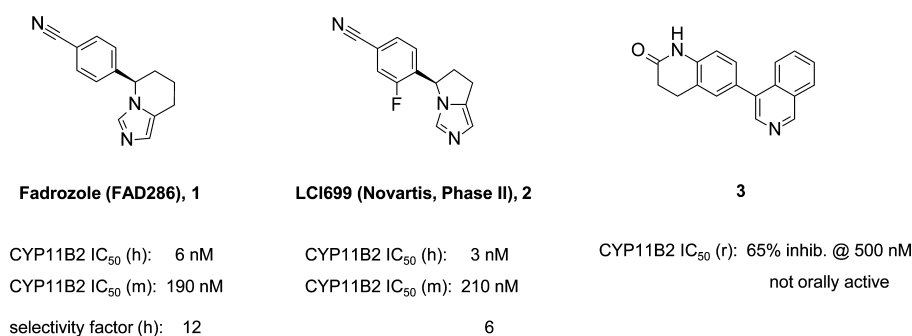CYP11B2 IC$_{50}$ (r): 65% inhib. @ 500 nM

not orally active

Figure 1. Aldosterone synthase inhibition was tested in renal leiomyoblastoma cells, ectopically expressing human (h), mouse (m), or rat (r) CYP11B2 or CYP11B1. All values are the mean of at least three experiments with a standard deviation of usually <25%. The selectivity factor (SF) is defined as the ratio between the IC$_{50}$ values on human CYP11B1 and CYP11B2.

first initial decline, return to pathological levels.[1,2] It has been demonstrated that the deleterious consequences of inappropriately increased aldosterone levels can be minimized by aldosterone blockade with mineralocorticoid receptor antagonists.[4−6] A direct inhibition of aldosterone synthesis is expected to provide even better protection, as it will also reduce nongenomic effects of aldosterone. Aldosterone, regulated by the RAAS, plays a central role in fluid and electrolyte homeostasis and is therefore one of the principal regulators of blood pressure.[7,8]

Aldosterone is a steroid hormone belonging to the mineralocorticoid family that is synthesized from cholesterol through a cascade of linear transformations mainly catalyzed by enzymes of the cytochrome P450 family.[9] The last three steps in this sequence are mediated by aldosterone synthase (CYP11B2), an enzyme that is mainly present in adrenal gland zona glomerulosa cells and to a lower extent in other tissues and is exclusively involved in the synthesis of aldosterone.[10] Thus, CYP11B2 qualifies as a primary target for the development of selective aldosterone synthesis inhibitors. Human CYP11B2 shows a high sequence identity of approximately 93% to 11β-hydroxylase (CYP11B1), an enzyme that is critical for the synthesis of cortisol and is mainly present in the zona fasciculata/reticularis.[11] A further considerable obstacle to the development and pharmacodynamic characterization of selective CYP11B2 inhibitors is encountered in the rather high species difference between human and rodent enzymes. For instance, rat CYP11B2 and human CYP11B2 display an overall sequence homology of only 68%, making it challenging to develop aldosterone synthase inhibitors with comparable potency on both species.[11] The nonselective CYP11B2 inhibitor FAD286 (1, Figure 1), which is the (+)-enantiomer of the aromatase inhibitor Fadrozole originally introduced in Japan for the treatment of breast cancer, and the mineralocorticoid antagonist spironolactone were evaluated in a rat model of chronic kidney disease.[12] Specifically angiotensin II and high salt treatment caused albuminuria, azotemia, renovascular hypertrophy, glomerular injury, tubulointerstitial fibrosis, and increased plasminogen activator inhibitor 1 (PAI-1) and expression of osteopontin mRNA. Both experimental compounds prevented these renal effects and attenuated cardiac and aortic medial hypertrophy. Following a 4-week treatment period with FAD286 (1), plasma aldosterone concentration was reduced, whereas spironolactone increased aldosterone levels after 4 and 8 weeks of treatment due to a compensatory mechanism. Similarly, spironolactone only, but not FAD286 (1), enhanced angiotensin II levels and

salt-stimulated PAI-1 mRNA expression in both aorta and heart. In other studies the CYP11B2 inhibitor FAD286 (1) only slightly improved blood pressure but improved cardiovascular function and ameliorated cardiac hypertrophy, albuminuria, cell infiltration, and matrix deposition in the heart and kidney in rats with experimental heart failure.[13]

Recently, Novartis reported clinical data on the first administration of LCI699 (2, Figure 1), an orally active CYP11B2 inhibitor structurally closely related to FAD286 (1), to patients with primary aldosteronism (PA).[14,15] After a 2-week placebo run-in phase, patients were orally dosed with 0.5 mg b.i.d. of LCI699 (2) for 2 weeks, followed by 1.0 mg b.i.d. of LCI699 (2) for 2 weeks and a placebo for 1 additional week. The authors concluded that the administration of 2, up to a dose of 1.0 mg b.i.d., inhibited CYP11B2 effectively and safely in patients with PA, resulting in significantly reduced levels of aldosterone in both plasma and urine. The treatment resulted in a rapid correction of hypokalemia and a modest decrease in blood pressure. As a consequence of the low selectivity against CYP11B1, biological signs of partial inhibition of cortisol synthesis such as dose-dependent increases in both plasma adrenocorticotropic hormone (ACTH) and 11-deoxycortisol (precursor of cortisol synthesis) concentrations were observed. In summary, these data support the concept that a CYP11B2 inhibitor can lower inappropriately high aldosterone levels and thus might be an interesting target for the treatment of hypertension and renal disorders. However, good selectivity against CYP11B1 is critical in order to prevent undesired side effects related to the hypothalamic−pituitary−adrenal (HPA) axis.

This clearly illustrates that there is a need for more potent, selective, and orally active CYP11B2 inhibitors for both proof-of-concept studies in translational animal models and treatment in man. The imidazole-type inhibitors FAD286 (1) and LCI699 (2) are potent compounds in man but considerably less potent in rodents. Furthermore, both also show a lack of selectivity against human CYP11B1. The recently disclosed isoquinoline compound 3 from Hartmann et al. is a non-imidazole-type CYP11B2 inhibitor potent against rat aldosterone synthase but unfortunately not suitable for oral application in rodents (Figure 1).[16]

Herein we report on our aldosterone synthase inhibitor drug discovery program to identify compounds with excellent potency and an improved selectivity profile that are suitable for oral application and would enable the study of biological effects of aldosterone synthase inhibition in both rodents and non-human primates.

Scheme 1. Synthesis of Aldosterone Synthase Tetrahydroisoquinoline Inhibitors 5–11[a]
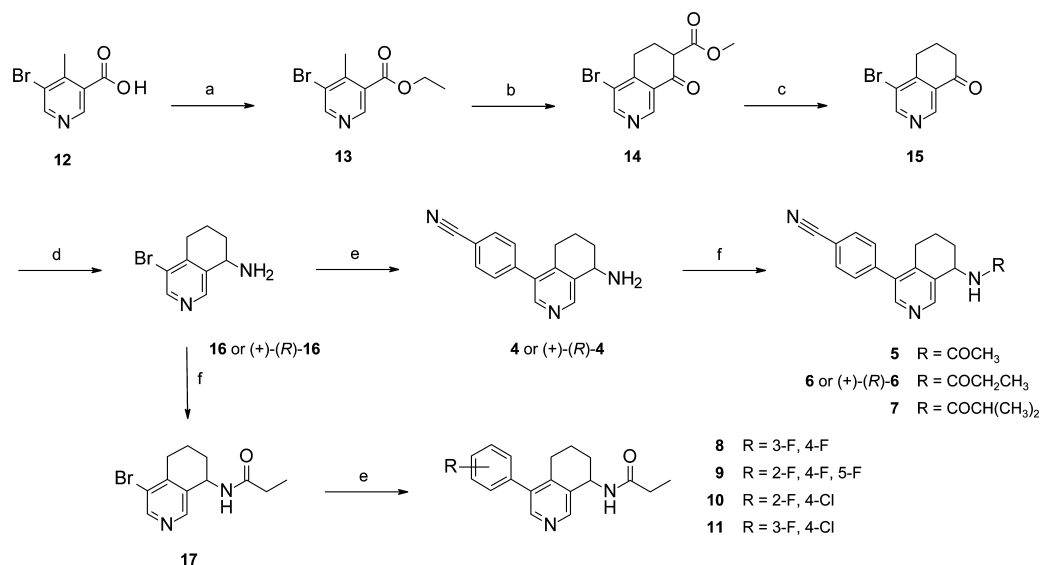
[a]Reagents and conditions: (a) EtOH, EDCI, DMAP, CH₂Cl₂, rt, 16 h, 84%; (b) (i) *n*-BuLi, *N,N*-diisopropylamine, −78 °C; (ii) methyl acrylate, −78 °C, 2.5 h, 95% (70% purity); (c) 6 N aqueous HCl, reflux, 2.5 h, 69%; (d) **16**: Ti(O*i*-Pr)₄, 2 M NH₃ in MeOH, NaBH₄, rt, 7 h, 85%. (+)-(*R*)-**16**: (i) Ti(O*i*-Pr)₄, 2 M NH₃ in MeOH, NaBH₄, rt, 7 h, 85%; (ii) Chiralpak AD column (40% isopropanol in *n*-heptane). (−)-(*S*)-**16**, 37% and (+)-(*R*)-**16**, 36%; (e) boronic acid, Pd(Ph₃)₄, Na₂CO₃, EtOH, H₂O, 85 °C, 16 h. **4**: with 4-cyanophenylboronic acid, 81%. (+)-(*R*)-**4**: with 4-cyanophenylboronic acid, 84%. **8**: with 3,4-difluorophenylboronic acid, 85%. **9**: with 2,4,5-trifluorophenylboronic acid, 40%. **10**: with 4-chloro-2-fluorophenylboronic acid, 70%. **11**: with 4-chloro-3-fluorophenylboronic acid, 83%; (f) **5**: acetyl chloride, triethylamine, CH₂Cl₂, −20 °C, 30 min, 44%. **6**: propionic acid, EDCI, CH₂Cl₂, rt, 16 h, 95%. (+)-(*R*)-**6**: propionic acid, EDCI, CH₂Cl₂, rt, 16 h, 81%. **7**: isobutyryl chloride, triethylamine, CH₂Cl₂, −20 °C, 30 min, 63%.

■ CHEMISTRY

The synthesis of aldosterone synthase inhibitors **5–11** is outlined in Scheme 1. Esterification of commercially available 5-bromo-4-methylnicotinic acid (**12**) with ethanol under EDCI/DMAP activation provided ethyl ester **13**. Deprotonation of the methyl group with freshly prepared lithium diisopropylamide (LDA) followed by addition of methyl acrylate gave access to intermediate **14**. The first step in this domino reaction is the 1,4-Michael addition of the tolyl anion to the acrylate, followed by cyclization with the ethyl ester group to afford the cyclic keto ester **14**, which was isolated in a yield of 95% next to about 30% of unreacted starting material **13**.

The crude keto ester **14** was then engaged in a Krapcho decarboxylation using 6 M aqueous HCl to provide ketone **15**, which could easily be separated from hydrolyzed starting material **13** by chemical separation. Reductive amination of ketone **15** with ammonia in methanol in the presence of titanium(IV) isopropoxide and treatment with sodium borohydride furnished key building block **16**, which was central for preparation of both left- and right-hand-side variations of target compounds **5–11**. Suzuki reaction of aryl bromide compound **16** with 4-cyanophenylboronic acid provided access to tetrahydroisoquinoline amine **4**, which was then further reacted with different carboxyl acids to provide racemic inhibitors **5–7**. Similarly, amide formation of amine **16** with propionic acid yielded aryl bromide compound **17**, which was then reacted under Suzuki conditions with various phenyl-boronic acids to provide racemic target compounds **8–11** in good to excellent yields. Racemic compound (±)-**6** was separated by preparative chiral chromatography on a Chiralpak AD column into the two enantiomercially pure forms (+)-**6** and (−)-**6**. Attempts to assign the absolute configuration of the more potent enantiomer (+)-**6** by single crystal X-ray analysis

were not successful. Therefore, the absolute configuration of (+)-**6** was derived from X-ray crystallographic analysis of the undesired bromotetrahydroisoquinoline enantiomer (−)-**16**, which was determined to be of (*S*)-configuration (Figure 2).[17] In an analogous fashion the chiral separation of aminotetrahydroisoquinoline intermediate (±)-**16** enabled the direct formation of (+)-(*R*)-**6** from (+)-(*R*)-**16** using the synthetic route described above.
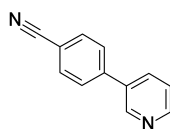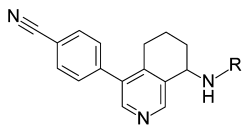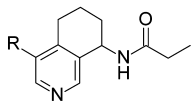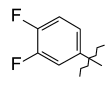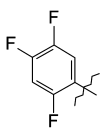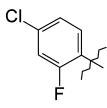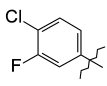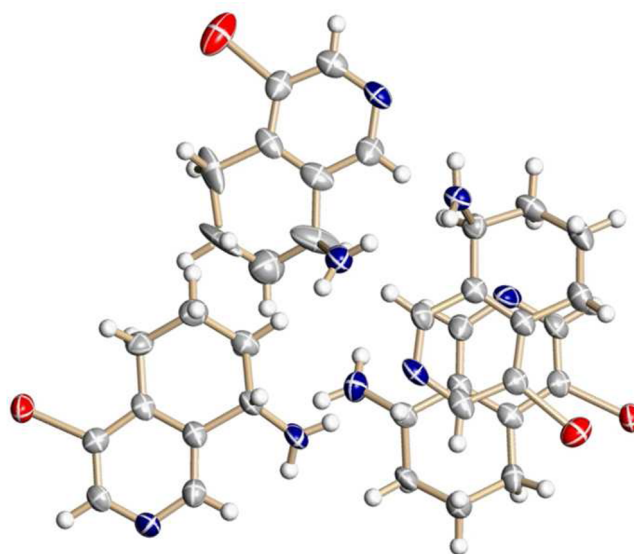

Figure 2. ORTEP drawing derived from the single crystal X-ray analysis of bromotetrahydroisoquinoline intermediate (−)-**16** reveals the chiral center to be of (*S*)-configuration. Ellipsoids are drawn at the 50% probability level.

Table 1. Structure−Activity Relationship (SAR) Data for Tetrahydroisoquinoline Derivatives 4−11 and 18

compound	R	CYP11B2 IC$_{50}$ (h) [nM]	selectivity factor (h)	microsomal CL (h) / (m) / (r) [µg min^{-1} mg^{-1} protein]
18	-	40	8	< 10 / 53 / < 10
4	H	42	5	< 10 / 12 / < 10
5	COCH$_3$	21	13	< 10 / < 10 / < 10
6	COCH$_2$CH$_3$	25	28	< 10 / < 10 / < 10
7	COCH(CH$_3$)$_2$	123	33	< 10 / < 10 / < 10
8	(3,4-difluorophenyl)	47	18	< 10 / 17 / 85
9	(2,4,5-trifluorophenyl)	27	42	< 10 / < 10 / 78
10	(4-chloro-2-fluorophenyl)	28	53	< 10 / 21 / 46
11	(4-chloro-3-fluorophenyl)	14	95	< 10 / 36 / 31

RESULTS AND DISCUSSION

Initial attempts to enhance selectivity against CYP11B1 in the Fadrozole-imidazole series proved challenging and prompted us to look out for suitable replacements of the imidazole moiety. To make use of potential heme-iron binding in CYP11B2, we compiled a library of in-house compounds containing heteroaromatic substructures featuring a nitrogen lone pair and without substitution α to the nitrogen atom. A focused screen of this library yielded pyridine compound **18** as a promising hit structure with high ligand efficiency, demonstrating that the imidazole unit can be replaced by a pyridine group with comparable potency (Table 1). However, the selectivity factor (SF), defined as the ratio between the IC$_{50}$ values on human CYP11B1 and B2, for this compound was measured to be 8 and thus offered no improvement over imidazole-type inhibitor **1** (SF = 12). In addition, the moderate metabolic stability of arylpyridine compound **18** in mouse microsomes limited the use of this compound for oral proof-of-concept experiments.

With the aim to identify potential selectivity pockets we generated homology models of CYP11B1 and B2, respectively, and modeled the binding mode of inhibitor **18**, assuming a critical iron−pyridine nitrogen interaction (Figure 3). This structural hypothesis indicated additional space at the 4,5-position of the pyridine moiety. As illustrated in Figure 3, there are several amino acid differences between CYP11B1 and B2 enzymes within the extended binding site. Although they are not exposed for direct ligand interaction, they might still affect
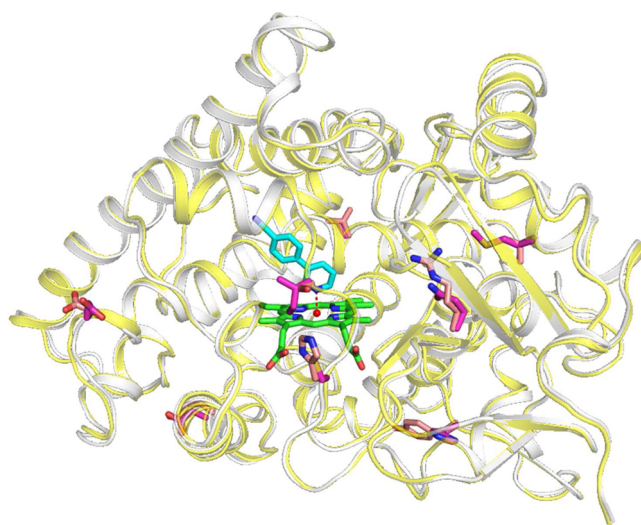

Figure 3. Homology models of CYP11B1 (white) and B2 (yellow) in cartoon representation. The heme cofactor is shown in green and modeled compound **18** in cyan. Amino acid differences within 16 Å of the modeled ligand are highlighted (B1, salmon; B2, magenta), which are at positions 68, V/M; 109, C/H; 112, I/S; 147, D/E; 302, E/D; 320, A/V; 404, Q/R; and 439, H/Y for CYP11B1/B2, respectively.[18]

details and plasticity of the binding region resulting in decent selectivity. Structure-guided design to fill the pocket on the

right-hand side prompted the synthesis of tetrahydroisoquinoline 4.

The tetrahydroisoquinoline 4 showed a potency of hCYP11B2 IC$_{50}$ = 42 nM together with a poor SF of 5 but revealed high stability in both human and rodent microsomes. Interestingly, amide bond formation at the free amino group in 4 was well tolerated providing acetylated and propionylated compounds 5 and 6 with a potency of IC$_{50}$ of 21 and 25 nM and improved selectivity values of SF of 13 and 28, respectively. Further enlargement of the alkyl substitution to an isopropyl side chain gave compound 7 with significantly inferior potency (IC$_{50}$ = 123 nM), albeit with a slightly improved selectivity factor of 33. In the isoquinoline series 5−7 log D values increased from 1.8 to 2.1 and 2.6,[19] concomitantly with an expected decrease in aqueous solubility from 415 to 360 and 90 μg mL^{-1}, respectively.[20] All three compounds 5−7 displayed high passive permeability in the Pampa assay (Pe > 4.4 × 10^{-6} cm s^{-1}),[21] low clearance in both human and rodent microsomes, and no inhibition of cytochrome P450 subtype enzymes 3A4, 2D6, and 2C9 (all IC$_{50}$ > 50 μM).

Having optimized the right-hand side of the molecule with respect to potency, selectivity, and rodent microsomal clearance, we next turned our attention to the optimization of the substitution pattern on the aryl ring. Exchange of the 4-cyanophenyl side chain in 6 to a 3,4-difluorophenyl motif provided compound 8 with reduced potency (IC$_{50}$ = 47 nM) and a slightly decreased selectivity factor of 18. Switching to a 2,4,5-trifluoro (9), 4-chloro-2-fluoro (10), and 4-chloro-3-fluoro (11) substitution pattern on the aryl ring resulted in a gain in potency (IC$_{50}$ of 27, 28, and 14 nM) and also improved selectivity to a SF of 42, 53, and 95, respectively. In the sequence 8−11 lipophilicity increased from log D of 3.0, 3.1 to 3.6 and 3.6 with aqueous solubility decreasing in the same order from 310, 239 to 129 and 99 μg mL^{-1}, respectively. Again, all compounds showed high passive permeability in the Pampa assay (Pe > 4.0 × 10^{-6} cm s^{-1}) and no inhibition of cytochrome P450 subtype enzymes 3A4, 2D6, and 2C9. Although tetrahydroisoquinoline 11 was found to be the most potent and selective compound in the entire series, and thus seemed to be an attractive candidate for further evaluation, the decreased rodent microsomal stability precluded its further evaluation. Similarly, compound 9 which showed an acceptable selectivity profile was not further considered due to poor rat microsomal stability. Finally, on the basis of the overall profile, tetrahydroisoquinoline 6 was selected for chiral separation owing to its good potency in combination with medium selectivity, high microsomal stability, and a balanced physicochemical profile (lipophilicity, log D = 2.1; permeability, Pe = 5.2 × 10^{-6} cm s^{-1}; solubility, 360 μg mL^{-1}). The separated enantiopure isomers of 6 showed significantly different affinities on hCYP11B2, with the (+)-enantiomer being 105-fold more potent than the (−)-enantiomer (Figure 4). The enantiomerically pure compound (+)-(R)-6 displayed not only single digit nanomolar potency on human aldosterone synthase (IC$_{50}$ = 9 nM) but was also very active on the cynomolgus monkey enzyme (IC$_{50}$ = 3 nM), with an attractive selectivity factor of 160 against CYB11B1 in the latter species. Similar to racemic 6 the physicochemical profile of (+)-(R)-6 was very attractive (log D = 2.2, Pe = 4.8 × 10^{-6} cm s^{-1}, solubility of 315 μg mL^{-1}), making it an interesting candidate for in vivo proof-of-concept studies.

Figure 5 shows the X-ray structure of human CYP11B2 in complex with inhibitor 11. Despite the limited resolution of 3.2
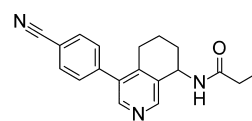
	(+)-(R)-6	(-)-(S)-6	
CYP11B2 IC$_{50}$ (h / c):	9 / 3 nM	942 / - nM	
selectivity factor (h / c):	22 / 160	9 / -	
CYP11B2 IC$_{50}$ (m):	530 nM	> 10 μM	
microsomal CL (h / m / r):	all < 10	all < 10	μg min^{-1} mg^{-1} protein
CYPs (3A4 / 2D6 / 2C9):	> 50 μM	> 20 μM	

Figure 4. In vitro data of tetrahydroisoquinoline enantiomers 6. Aldosterone synthase inhibition was tested in renal leiomyoblastoma cells, ectopically expressing human (h), cynomolgus monkey (c), mouse (m), or rat (r) CYP11B2 or CYP11B1. All values are the mean of at least three experiments with a standard deviation of usually <25%. The selectivity factor (SF) is defined as the ratio between the IC$_{50}$ values on human CYP11B1 and CYP11B2.
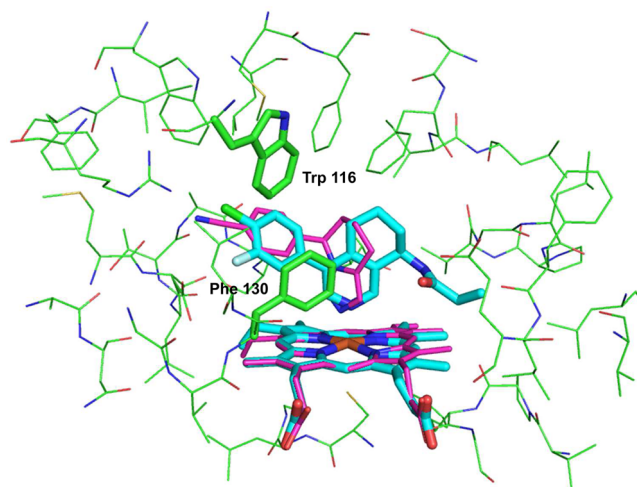

Figure 5. X-ray structure of hCYP11B2 with compound 11 (PDB code 4ZGX). The protein is displayed in green and the heme and the tetrahydroisoquinoline 11 in cyan sticks. Overlaid onto this structure are heme and Fadrozole from the complex structure with hCYP11B2 (magenta, PDB code 4FDH).[22]

Å, several features of the binding mode such as the close contact of the heme iron with the nitrogen lone pair of the tetrahydroisoquinoline core ($d \approx 2.0$ Å) and the orientation of the ligand in the binding site are unambiguous conclusions from the electron density. The crystal structure confirms the inhibitor binding mode as predicted by our homology model and therefore further validates the original design strategy. However, the absolute stereoconfiguration of the chiral center in compound 11 could not be resolved. Figure 5 also displays an overlay with the X-ray complex structure of Fadrozole with hCYP11B2, which became recently available.[22] The structure reveals that the iron interaction with the imidazole lone pair of Fadrozole is analogous to that with the tetrahydroisoquinoline nitrogen in our series and that the phenyl substituent occupies a similar position in both structures, engaging in aromatic interactions with the side chains of Trp116 and Phe130.

The tetrahydroisoquinoline (+)-(R)-6 showed an IC$_{50}$ of 530 nM on CYP11B2 in mouse and thus is of comparable potency with 3,4-dihydro-1H-quinolin-2-one 3 and about half the potency of reference compounds 1 or 2. However, the higher
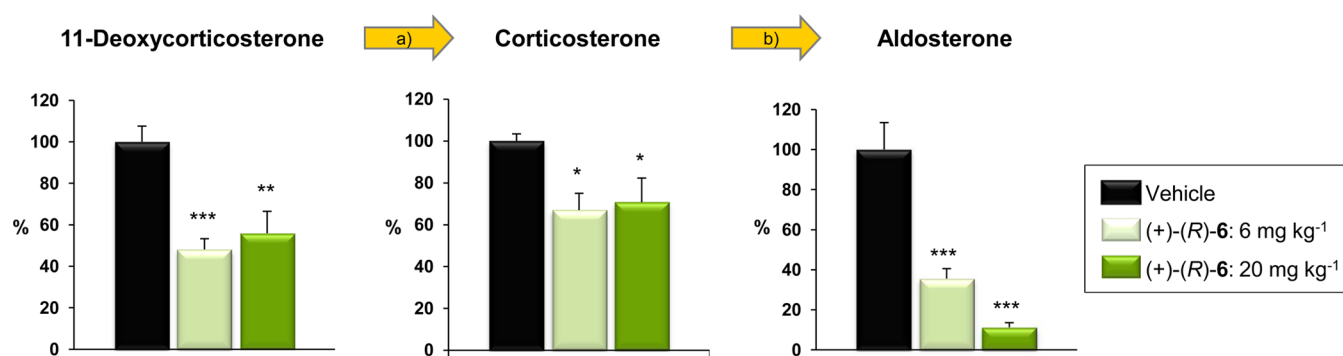
Figure 6. Lowering of aldosterone levels in db/db mice after food admix treatment with tetrahydroisoquinoline $(+)$-(R)-**6** for 21 days at doses of 6 and 20 mg kg^{-1}. Steroid levels are presented as % vs vehicle. Data are expressed as the mean $\pm$ SEM with $n = 10$ mice per group. Statistical analysis was performed by ANOVA followed by post hoc test: (∗) $p < 0.05$, (∗∗) $p < 0.01$, or (∗∗∗) $p < 0.001$ between control and the indicated test group. (a) Enzymatic step mediated by both CYP11B1 and CYP11B2. (b) Enzymatic step mediated by CYP11B2 only.
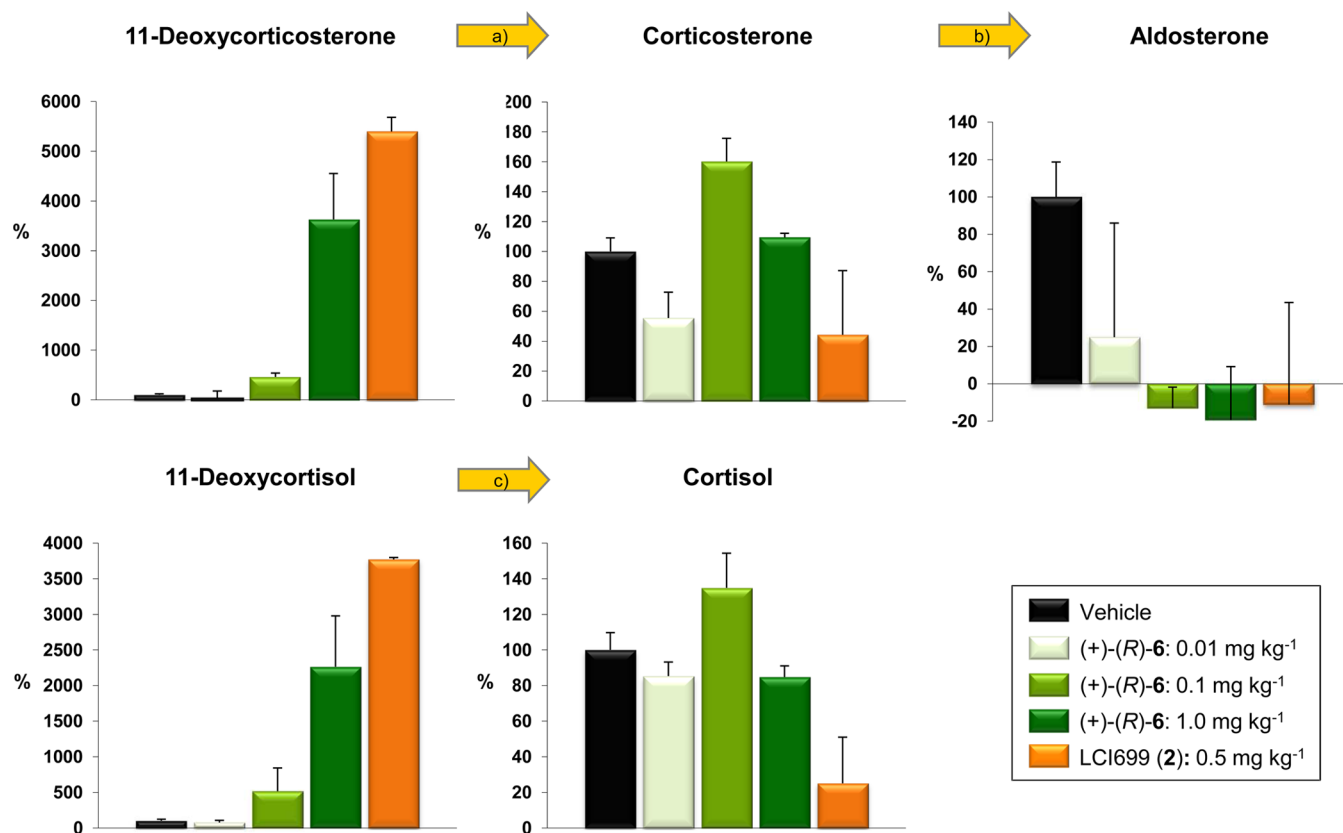

Figure 7. Steroid profile in cynomolgus monkey 60 min after ACTH challenge and treatment with tetrahydroisoquinoline $(+)$-(R)-**6**. Due to the natural variations of steroid levels of the individual animals, steroid baseline levels of each group at $t = 0$ were normalized to 0. The mean differences at $t = 60$ min are reported as % change vs vehicle (mean $\pm$ SEM with $n = 2$ monkeys per group except for vehicle with $n = 7 \times 2$ animals). Note that this mathematical transformation might render mean values below 0. (a) Enzymatic step mediated by both CYP11B1 and CYP11B2. (b) Enzymatic step mediated by CYP11B2 only. (c) Enzymatic step mediated by CYP11B1 only.

metabolic stability makes $(+)$-(R)-**6** the first selective compound suitable for oral dosing in mouse. Despite significant effort, it was not possible to establish a reliable in vitro expression and assay system for measuring mouse and rat CYP11B1 inhibition. Therefore, we assessed efficacy and selectivity of compound $(+)$-(R)-**6** directly in obese diabetic db/db mice, a well-known mouse model displaying constitutively elevated steroid levels.[23,24] Since both CYP11B1 and CYP11B2 catalyze the oxidation of 11-deoxycorticosterone to corticosterone, but only CYP11B2 can oxidize corticosterone to aldosterone, the selectivities of inhibition can be inferred from

analysis of the levels of these steroids. A prerequisite for this study was the accurate and concurrent measurement of a panel of up to seven steroid concentrations in plasma samples, which was accomplished by a highly optimized LC−MS−MS analysis protocol (for detailed information, see Supporting Information). At doses of 6 and 20 mpk (food admix, 21 days) significant and dose-dependent reduction of aldosterone plasma levels with no concurrent increase of 11-deoxycorticosterone, demonstrating selective inhibition of CYP11B2, was observed (Figure 6). In a similar experiment, where db/db mice were treated with a single dose (po) of 3 and 30 mg kg^{-1} of

unselective inhibitor LCI699 (**2**), precursor 11-deoxycorticos-terone showed at $t = 2$ h a dramatic 14- and 59-fold increase, respectively. In parallel, LCI699 (**2**) lowered both aldosterone and corticosterone levels (aldosterone to 51% and 37% of control, corticosterone to 29% and 9% of control; Figure S1 in Supporting Information). Together these results underscore the superiority of compound (+)-(*R*)-**6** for future in vivo assessment of aldosterone synthase blockage in rodent disease models.

On the basis of the encouraging mouse data, compound (+)-(*R*)-**6** was next tested in an angiotension II ZSF1 rat infusion model relevant for chronic kidney disease (20 mpk, food admix, 6 weeks) showing similarly a selective decrease of aldosterone production concomitant with an improvement in renal parameters (including albuminuria, glomerular filtration rate, and histology) to a better extent than the mineralocorti-coid receptor antagonist eplerenone.[25]

The relatively high selectivity factor of 160 for (+)-(*R*)-**6** in cynomolgus monkeys prompted us to test this compound also in primates in order to elucidate the effects on steroid profiles (Figure 7). In contrast to rodents, primates produce 11-deoxycortisol in addition to 11-deoxycorticosterone.[11] Since the conversion of 11-deoxycortisol to cortisol is only catalyzed by CYP11B1, this allowed an independent assessment of the selectivity of inhibition. Cynomolgus monekys were treated with (+)-(*R*)-**6** at doses of 0.01, 0.1, and 1.0 mg kg^{-1} and with reference compound LCI699 (**2**) at 0.5 mg kg^{-1} at $t = 0$. Adrenocorticotropic hormone (ACTH, Synacthen) was administred 5 min later. Although the hormone levels were measured over a time period of 6 h, percentage of changes were calculated 60 min after Synacthen application where c_{max} is observed and which is the clinically relevant time point (Table S1). An additional argument to evaluate the efficacy of compound (+)-(*R*)-**6** at the single time point $t = 60$ min rather than using steroid AUC_{0-6h} profiles is the natural variation of steroid levels observed during the day. The maximum decrease of aldosterone levels for compound (+)-(*R*)-**6** was obtained for both doses of 0.1 and 1.0 mg kg^{-1} which was comparable to the level observed with LCI699 (**2**) at a dose of 0.5 mg kg^{-1}. However, at a dose of 0.5 mg kg^{-1}, LCI699 (**2**) resulted in a clear reduction of cortisol levels with a concurrent build-up of 11-deoxycortisol precursor concen-trations. In contrast, tetrahydroisoquinoline (+)-(*R*)-**6** gave no decrease of cortisol levels at all levels investigated and only displayed an increase of plasma 11-deoxycortisol at the highest applied dose of 1.0 mg kg^{-1}; from this it was concluded that in vivo selectivity against CYP11B1 is seen up to a dose of at least 0.1 mg kg^{-1}. This experimental observation is in good accordance with PK measurements that showed that the free plasma levels measured for tetrahydroisoquinoline (+)-(*R*)-**6** at doses of ≤0.1 mg kg^{-1} are significantly below the IC_{50} against cytochrome CYP11B1 corresponding to a calculated in vivo CYP11B1 inhibition of <10% (Table S2).

CONCLUSION

The novel tetrahydroisoquinoline compound (+)-(*R*)-**6** shows excellent inhibitory potency against human and cynomolgus monkey aldosterone synthase, with a remarkable selectivity factor of 160 against CYB11B1 in the latter species. The compound significantly lowered aldosterone plasma levels in a dose-dependent manner in mice and cynomolgus monkeys and protected kidney structure and function in a ZSF1 rat model of chronic kidney disease. In Synacthen challenged conscious

cynomolgus monkeys selectivity against CYP11B1 was demonstrated up to a dose of 0.1 mg kg^{-1} with complete inhibition of aldosterone synthesis. Although compound (+)-(*R*)-**6** displays only moderate activity in rodents, the high metabolic stability allows for oral application, making it a suitable tool compound for in vivo assessment of aldosterone synthase blockage in rodent disease models. The improved properties of tetrahydroisoquinoline (+)-(*R*)-**6** differentiate this compound from the recently published benzimidazole-type CYP11B2 inhibitors which were not suitable for evaluation in classical rodent models of aldosteronism due to their rather weak rat potency.[26]

■ EXPERIMENTAL SECTION

General Methods for Chemistry. Reactions were carried out under an atmosphere of argon. Solvents and reagents were obtained from commercial sources and were used without further purification. All reactions were monitored by thin-layer chromatography (TLC) on Merck silica gel 60 F$_{254}$ TLC glass plates (visualized by UV fluorescence at $\lambda = 254$ nm). ^{1}H nuclear magnetic resonance (NMR) spectra were recorded on a Bruker 300 or 600 MHz instrument. The respective ^{13}C NMR spectra were measured on a 150 MHz instrument. The chemical shifts (δ in ppm) are reported relative to tetramethylsilane as internal standard. Resonances in the ^{1}H NMR spectra are reported to the nearest 0.01 ppm. NMR abbreviations are as follows: s, singlet; d, doublet; t, triplet; q, quadruplet; m, multiplet; br, broad. The purity of final compounds as measured by LC−MS was at least >95%. Purity of compounds was analyzed by ^{1}H NMR and LC−MS. LC−MS spectra were recorded on a Waters UPLC−MS system equipped with Waters Acquity CTC PAL autosampler and a Waters SQD single quadrupole mass spectrometer. Analytical separation was conducted on a Zorbax Eclipse Plus C18 2.1 mm × 30 mm, 1.7 μm column at 50 °C; eluent A = 0.01% formic acid in water; eluent B = acetonitrile at a flow of 1 mL min^{-1}. Gradient: 0 min 3% B, 0.2 min 3% B, 2 min 97% B, 1.7 min 97% B, and 2.0 min 97% B. The injection volume was 2 μL. LC−MS high resolution spectra were recorded on an Agilent LC system consisting of an Agilent 1290 high pressure gradient system, a CTC PAL autosampler, and an Agilent 6520 QTOF. Analytical separation was achieved on a Zorbax Eclipse Plus C18 column (2.1 mm × 50 mm, 1.7 μm) at 55 °C; eluent A = 0.01% formic acid in water; eluent B = 0.01% formic acid in acetonitrile at a flow of 1 mL min^{-1}. Gradient: 0 min 5% B, 0.3 min 5% B, 4.5 min 99% B, and 5 min 99% B. The injection volume was 2 μL. Ionization was performed in multimode source. The mass spectrometer was run in 2 GHz extended dynamic range mode, resulting in a resolution of about 10 000 at $m/z = 922$. Mass accuracy was ensured by internal drift correction. Service measurements were performed by the NMR and MS service teams at F. Hoffmann-La Roche, Basel.

Representative Synthetic Procedures. Preparation of Ethyl 5-Bromo-4-methylnicotinate (13). To a stirred light brown suspension of 5-bromo-4-methylnicotinic acid (**12**, 10.00 g, 46.3 mmol) and ethanol (2.35 g, 2.97 mL, 50.9 mmol) in CH$_2$Cl$_2$ (231 mL) at 0 °C under argon were added EDCI (10.9 g, 55.5 mmol) and DMAP (566 mg, 4.63 mmol). Stirring was continued overnight and the reaction mixture allowed to warm to rt. The reaction mixture was poured on aqueous 10% KH$_2$PO$_4$ solution followed by extraction with EtOAc (3×). The organic phases were washed once with aqueous 10% KH$_2$PO$_4$, aqueous saturated NaHCO$_3$, and with aqueous saturated NaCl solution. The combined organic phases were dried over Na$_2$SO$_4$, filtered, and evaporated to afford the title compound (9.49 g, 84%) as brown solid. LC−MS: $t_R = 1.19$ min, 97% (265 nm); $t_R = 1.19$ min, 97% (225 nm). ^{1}H NMR (600 MHz, DMSO-d_6): $\delta = 8.86$ (s, 1H), 8.82 (s, 1H), 4.35 (q, $J = 7.1$ Hz, 2H), 2.58 (s, 3H), 1.33 (t, $J = 7.1$ Hz, 3H). ^{13}C NMR (150 MHz, DMSO-d_6): $\delta = 165.1$, 153.6, 149.0, 146.9, 128.4, 124.7, 61.6, 19.7, 14.0. HRMS (C$_9$H$_{10}$BrNO$_2$): calcd 242.9895; found 242.9898.

Preparation of Methyl 4-Bromo-8-oxo-5,6,7,8-tetrahydro-isoquinoline-7-carboxylate (14). Ethyl 5-bromo-4-methylnicotinate (**13**, 7.04 g, 28.8 mmol) in THF (28.8 mL) was added over a period of 20 min to a solution of LDA (31.7 mmol), which was freshly prepared from *N,N*-diisopropylamine (4.52 mL, 31.7 mmol) and *n*-BuLi (19.8 mL, 31.7 mmol; 1.6 M in hexane) in THF (144 mL) at −78 °C. The resulting dark red solution was stirred for 20 min, then methyl acrylate (6.5 mL, 72.1 mmol) in THF (28.8 mL) was added within 15 min. The reaction was stirred an additional 1.5 h, then aqueous 10% AcOH (57.8 mL, 101 mmol) was added (pH 4−5) and the reaction was allowed to warm to rt. After evaporation, the residue was partitioned between aqueous saturated NaHCO$_3$ and EtOAc, and extracted with EtOAc (3×). The combined organic phases were dried over Na$_2$SO$_4$ and concentrated to afford the title compound (7.80 g, 95% in 70% purity as keto−enol mixture and 30% of starting material **13**) as brown solid. The material was used crude in the consecutive reaction step without further purification. LC−MS: 280.0 ([M + H]$^+$, 1 Br).

Preparation of 4-Bromo-6,7-dihydroisoquinolin-8(5*H*)-one (15). The crude methyl 4-bromo-8-oxo-5,6,7,8-tetrahydro-isoquinoline-7-carboxylate (**14**, 7.79 g, 27.4 mmol) was dissolved (small amount of insoluble material remained) in aqueous 6 M HCl (84.1 mL, 505 mmol) and heated at reflux for 2.5 h (dark brown solution, no more SM visible on TLC). The acidic solution was concentrated in vacuo, suspended in water (∼25 mL), cooled in an ice bath, and basified with 6.0 M KOH. The aqueous solution was washed with diethyl ether (2×) and CH$_2$Cl$_2$ (3×), and the combined organic layers were dried over Na$_2$SO$_4$, filtered, and concentrated to afford the title compound (4.30 g, 69%) as brown solid. LC−MS: t_R = 1.08 min, 97% (265 nm); t_R = 1.08 min, 97% (225 nm). ^{1}H NMR (300 MHz, DMSO-d_6): δ = 8.89 (s, 1H), 8.88 (s, 1H), 2.95 (dd, J = 6.1 Hz, 2H), 2.66 (dd, J = 7.5, 5.9 Hz, 2H), 2.21−2.02 (m, 2H). ^{13}C NMR (150 MHz, DMSO-d_6): δ = 196.7, 154.3, 151.9, 146.7, 129.2, 122.6, 37.6, 28.6, 20.9. HRMS (C$_9$H$_8$BrNO): calcd 224.9789; found 224.9789.

Preparation of (*rac*)-4-Bromo-5,6,7,8-tetrahydroisoquinolin-8-amine (16). 4-Bromo-6,7-dihydroisoquinolin-8(5*H*)-one (**15**, 4.81g, 21.3 mmol), titanium(IV) isopropoxide (12.5 mL, 42.6 mmol), and ammonia (53.2 mL, 106 mmol; 2.0 M solution in MeOH) were stirred at rt for 5 h. The reaction was cooled to 0 °C, NaBH$_4$ (1.21 g, 31.9 mmol) added portionwise over 10 min, and the resulting mixture stirred at rt for an additional 2 h. The reaction was quenched by pouring it into aqueous ammonium hydroxide (25%) and the formed precipitate filtered and washed with EtOAc (3×, each time suspended in EtOAc and stirred for 5 min). The organic layer was separated, and the remaining aqueous layer was extracted with EtOAc. The combined organic phases were extracted with 1 M HCl. The acidic aqueous layer was washed with EtOAc (1×), then treated with aqueous sodium hydroxide (2 M) to give pH 10−12 and extracted with EtOAc (3×). The combined second organic extracts were washed with brine, dried over Na$_2$SO$_4$, and concentrated in vacuo to give the title compound (4.11 g, 85%) as brown solid. LC−MS: t_R = 0.26 min, 89% (265 nm); t_R = 0.26 min, 91% (225 nm). ^{1}H NMR (600 MHz, DMSO-d_6): δ = 8.59 (s, 1H), 8.48 (s, 1H), 3.92 (t, J = 5.7 Hz, 1H), 2.70−2.63 (m, 1H), 2.62−2.56 (m, 1H), 1.98−1.90 (m, 1H), 1.87−1.81 (m, 1H), 1.75−1.66 (m, 1H), 1.63−1.55 (m, 1H). ^{13}C NMR (150 MHz, DMSO-d_6): δ = 149.1, 148.1, 144.6, 140.1, 122.7, 46.9, 31.7, 29.3, 18.1. HRMS (C$_9$H$_{11}$BrN$_2$): calcd 226.0106; found 226.0107.

Preparation of (+)-(*R*)-4-Bromo-5,6,7,8-tetrahydro-isoquinolin-8-amine ((+)-(*R*)-16) and (−)-(*S*)-4-Bromo-5,6,7,8-tetrahydroisoquinolin-8-amine ((−)-(*S*)-16). The two enantiomers of **16** (300 mg) were separated on a Chiralpak AD column (40% isopropanol in *n*-heptane) to give (+)-(*R*)-**16** (109 mg, 36%) and (−)-(*S*)-**16** (112 mg, 37%) as light brown crystals.

Enantiomer (+)-(*R*)-**16**. LC−MS: t_R = 0.92 min, 94% (265 nm); t_R = 0.92 min, 96% (220 nm). ^{1}H NMR (600 MHz, DMSO-d_6): δ = 8.59 (s, 1H), 8.48 (s, 1H), 3.92 (t, J = 5.7 Hz, 1H), 2.70−2.63 (m, 1H), 2.62−2.56 (m, 1H), 1.98−1.90 (m, 1H), 1.87−1.81 (m, 1H), 1.75−1.66 (m, 1H), 1.63−1.55 (m, 1H). ^{13}C NMR (150 MHz, DMSO-d_6): δ = 149.0, 148.1, 144.6, 140.1, 122.7, 46.9, 31.6, 29.3, 18.0. HRMS

(C$_9$H$_{11}$BrN$_2$): calcd 226.0106; found 226.0104. $[\alpha]^{20}_D$ +8.00 (*c* 1.0, MeOH).

Enantiomer (−)-(*S*)-**16**. LC−MS: t_R = 0.92 min, 89% (265 nm); t_R = 0.92 min, 94% (220 nm). ^{1}H NMR (600 MHz, DMSO-d_6): δ = 8.59 (s, 1H), 8.48 (s, 1H), 3.92 (t, J = 5.7 Hz, 1H), 2.70−2.63 (m, 1H), 2.62−2.56 (m, 1H), 1.98−1.90 (m, 1H), 1.87−1.81 (m, 1H), 1.75−1.66 (m, 1H), 1.63−1.55 (m, 1H). ^{13}C NMR (150 MHz, DMSO-d_6): δ = 149.0, 148.1, 144.6, 140.1, 122.7, 46.9, 31.6, 29.3, 18.0. HRMS (C$_9$H$_{11}$BrN$_2$): calcd 226.0106; found 226.0104. $[\alpha]^{20}_D$ −8.72 (*c* 0.41, MeOH). Crystallization from *n*-pentane followed by recrystallization from *n*-heptane provided single crystals suitable for X-ray crystallographic analysis.

Preparation of (*rac*)-N-(4-Bromo-5,6,7,8-tetrahydro-isoquinolin-8-yl)propionamide (17). To a stirred black solution of (*rac*)-4-bromo-5,6,7,8-tetrahydroisoquinolin-8-amine (**16**, 317 mg, 1.4 mmol) and propionic acid (115 μL, 1.54 mmol) in CH$_2$Cl$_2$ (7.0 mL) at 0 °C was added EDCI (295 mg, 1.54 mmol). Stirring was continued overnight and the reaction mixture allowed to warm to rt. The reaction mixture was poured on aqueous 10% KH$_2$PO$_4$ solution followed by extraction with EtOAc (3×). The organic phases were washed once with aqueous 10% KH$_2$PO$_4$, aqueous saturated NaHCO$_3$, and aqueous saturated NaCl solution. The organic phase was dried over Na$_2$SO$_4$, filtered, evaporated, and purified by precipitation from CH$_2$Cl$_2$ with *n*-pentane to afford the title compound (365 mg, 92%) as light brown solid. LC−MS: t_R = 1.42 min, 92% (265 nm); t_R = 1.42 min, 91% (225 nm). ^{1}H NMR (600 MHz, DMSO-d_6): δ = 8.54 (s, 1H), 8.29 (s, 1H), 8.23 (d, J = 8.5 Hz, 1H), 5.05−5.01 (m, 1H), 2.69−2.64 (m, 2H), 2.13 (quin, J = 7.4 Hz, 2H), 1.92−1.87 (m, 1H), 1.84 (br dd, J = 5.0, 2.5 Hz, 1H), 1.83−1.76 (m, 1H), 1.72−1.67 (m, 1H), 1.03 (t, J = 7.6 Hz, 3H). ^{13}C NMR (150 MHz, DMSO-d_6): δ = 172.5, 148.8, 148.6, 145.5, 136.4, 122.8, 44.2, 29.0, 28.5, 28.4, 18.6, 10.0. HRMS (C$_{12}$H$_{15}$BrN$_2$O): calcd 282.0368; found 282.0372.

Preparation of (*rac*)-4-(8-Amino-5,6,7,8-tetrahydro-isoquinolin-4-yl)benzonitrile (4). (*rac*)-4-Bromo-5,6,7,8-tetrahydroisoquinolin-8-amine (**16**, 681 mg, 3 mmol) and 4-cyanophenylboronic acid (540 mg, 3.6 mmol) were dissolved in ethanol (54 mL) to give a light brown solution. Na$_2$CO$_3$ (350 mg, 3.3 mmol) dissolved in water (8.9 mL) was added followed by tetrakis(triphenylphosphine)palladium (0) (104 mg, 90 μmol) after evacuation and replacing with argon (cycle repeated 5×). The solution was then heated at 85 °C overnight. The reaction was treated with an aqueous 10% NaCl solution and extracted with EtOAc (3×). The organic phases were washed again with an aqueous 10% NaCl solution, dried over Na$_2$SO$_4$, filtered, and evaporated under reduced pressure to give a brown foam which was purified by flash chromatography [50 g SiO$_2$, Telos cartridge, CH$_2$Cl$_2$/MeOH (5% → 7.5%)] and precipitation from CH$_2$Cl$_2$ with *n*-pentane. The title compound (605 mg, 81%) was isolated as a light brown foam. LC−MS: t_R = 0.98 min, 99% (265 nm); t_R = 0.98 min, 98% (225 nm). ^{1}H NMR (300 MHz, DMSO-d_6): δ = 8.69 (s, 1H), 8.18 (s, 1H), 7.94 (d, J = 8.1 Hz, 2H), 7.58 (d, J = 8.1 Hz, 2H), 3.98 (dd, J = 5.4 Hz, 1H), 2.47−2.29 (m, 2H), 2.00−1.72 (m, 2H), 1.70−1.49 (m, 2H). ^{13}C NMR (150 MHz, DMSO-d_6): δ = 150.3, 146.5, 142.7, 142.6, 137.1, 134.6, 132.3, 130.4, 118.7, 110.5, 46.9, 31.9, 27.0, 18.5. HRMS (C$_{16}$H$_{15}$N$_3$): calcd 249.1266; found 249.1268.

Preparation of (+)-4-[(8*R*)-8-Amino-5,6,7,8-tetrahydro-isoquinolin-4-yl]benzonitrile ((+)-(*R*)-4). (+)-(*R*)-4-Bromo-5,6,7,8-tetrahydroisoquinolin-8-amine ((+)-(*R*)-**16**, 90.8 mg, 400 μmol) and 4-cyanophenylboronic acid (72 mg, 480 μmol) were dissolved in ethanol (7.1 mL) to give a light brown solution. Na$_2$CO$_3$ (46.6 mg, 440 μmol) dissolved in water (0.8 mL) was added followed by tetrakis(triphenylphosphine)palladium (0) (13.9 mg, 12 μmol) after evacuation and replacing with argon (cycle repeated 5×). The solution was then heated at 85 °C overnight. The reaction was treated with an aqueous 10% NaCl solution and extracted with EtOAc (3×). The organic phases were washed again with an aqueous 10% NaCl solution, dried over Na$_2$SO$_4$, filtered, and evaporated under reduced pressure to give a brown foam which was purified by flash chromatography [20 g SiO$_2$, Telos cartridge, CH$_2$Cl$_2$/MeOH (5% → 10%)] and precipitation from CH$_2$Cl$_2$ with *n*-pentane. The title

compound (84 mg, 84%) was isolated as a light yellow foam. LC–MS: t_R = 0.98 min, 99% (265 nm); t_R = 0.98 min, 98% (225 nm). ^{1}H NMR (300 MHz, DMSO-d_6): δ = 8.69 (s, 1H), 8.18 (s, 1H), 7.94 (d, J = 8.1 Hz, 2H), 7.58 (d, J = 8.1 Hz, 2H), 3.98 (dd, J = 5.4 Hz, 1H), 2.47–2.29 (m, 2H), 2.00–1.72 (m, 2H), 1.70–1.49 (m, 2H). ^{13}C NMR (150 MHz, DMSO-d_6): δ = 150.3, 146.5, 142.7, 142.6, 137.1, 134.6, 132.3, 130.4, 118.7, 110.5, 46.9, 31.9, 27.0, 18.5. HRMS ($C_{16}H_{15}N_3$): calcd 249.1266; found 249.1268.

Preparation of (rac)-N-(4-(4-Cyanophenyl)-5,6,7,8-tetrahydroisoquinolin-8-yl)acetamide (5). A solution of (rac)-4-(8-amino-5,6,7,8-tetrahydroisoquinolin-4-yl)benzonitrile (4, 62.3 mg, 250 μmol) in CH_2Cl_2 (3.6 mL) cooled to −20 °C was treated with acetyl chloride (21.3 μL, 275 μmol) and triethylamine (41.8 μL, 300 μmol). After 30 min, an additional drop of acetyl chloride was added, and after 5 min the mixture was treated with MeOH (0.2 mL) and extracted with water/EtOAc (3×). The organic phases were dried over Na_2SO_4, filtered, and evaporated under reduced pressure. Purification by flash chromatography [50 g SiO_2, Telos cartridge, CH_2Cl_2/MeOH (2% → 3%)] and precipitation from CH_2Cl_2 with n-pentane gave the title compound (32 mg, 44%) as an off-white powder. LC–MS: t_R = 1.18 min, 96% (265 nm); t_R = 1.18 min, 96% (225 nm). ^{1}H NMR (300 MHz, DMSO-d_6): δ = 8.41 (s, 1H), 8.36 (d, J = 8.5 Hz, 1H), 8.25 (s, 1H), 7.95 (d, J = 8.5 Hz, 2H), 7.59 (d, J = 8.5 Hz, 2H), 5.09 (ddd, J = 7.3 Hz, 1H), 2.60–2.53 (m, 2H), 1.95–1.85 (m, 1H), 1.89 (s, 3H), 1.81–1.62 (m, 3H). ^{13}C NMR (150 MHz, DMSO-d_6): δ = 168.7, 149.9, 147.0, 143.7, 142.2, 134.8, 133.8, 132.4, 130.4, 118.7, 110.7, 44.3, 28.9, 26.8, 22.7, 19.0. HRMS ($C_{18}H_{17}N_3O$): calcd 291.1372; found 291.1376.

Preparation of (rac)-N-(4-(4-Cyanophenyl)-5,6,7,8-tetrahydroisoquinolin-8-yl)propionamide (6). To a stirred solution of (rac)-4-(8-amino-5,6,7,8-tetrahydroisoquinolin-4-yl)benzonitrile (4, 480 mg, 1.93 mmol) and propionic acid (158 μL, 2.12 mmol) in CH_2Cl_2 (10 mL) at 0 °C under argon was added EDCI (406 mg, 2.12 mmol). Stirring was continued overnight, and the reaction mixture was allowed to warm to rt. The reaction mixture was poured into aqueous 10% KH_2PO_4 solution followed by extraction with EtOAc (3×). The organic phases were washed once with aqueous 10% KH_2PO_4, aqueous saturated $NaHCO_3$, and aqueous saturated NaCl solution. The organic phase was dried over Na_2SO_4, filtered, and evaporated to afford the title compound (558 mg, 95%) as light brown solid. LC–MS: t_R = 1.56 min, 97% (265 nm); t_R = 1.18 min, 98% (225 nm). ^{1}H NMR (300 MHz, DMSO-d_6): δ = 8.39 (s, 1H), 8.28 (d, J = 8.5 Hz, 1H), 8.24 (s, 1H), 7.95 (d, J = 8.5 Hz, 2H), 7.59 (d, J = 8.3 Hz, 2H), 5.10 (ddd, J = 6.5 Hz, 1H), 2.59–2.54 (m, 2H), 2.15 (qd, J = 7.6, 2.9 Hz, 2H), 1.96–1.82 (m, 1H), 1.81–1.62 (m, 3H), 1.05 (t, J = 7.6 Hz, 3H). ^{13}C NMR (150 MHz, DMSO-d_6): δ = 172.5, 149.8, 147.0, 143.6, 142.2, 134.8, 133.9, 132.4, 130.3, 118.7, 110.7, 44.2, 28.9, 28.5, 26.8, 19.0, 10.0. HRMS ($C_{19}H_{19}N_3O$): calcd 305.1528; found 305.1537.

Preparation of (+)-(R)-N-(4-(4-Cyanophenyl)-5,6,7,8-tetrahydroisoquinolin-8-yl)propionamide ((+)-(R)-6) and (−)-(S)-N-(4-(4-Cyanophenyl)-5,6,7,8-tetrahydroisoquinolin-8-yl)propionamide ((−)-(S)-6). The two enantiomers of 6 (548 mg) were separated on a Chiralpak AD column (30% isopropanol in n-heptane) to give after precipitation from CH_2Cl_2 with n-pentane (+)-(R)-6 (202 mg, 37%) and (−)-(S)-6 (125 mg, 36%) as off-white solids.

Enantiomer (+)-(R)-6. LC–MS: t_R = 1.59 min, 100% (265 nm); t_R = 1.59 min, 99% (220 nm). ^{1}H NMR (600 MHz, DMSO-d_6): δ = 8.39 (s, 1H), 8.28 (d, J = 8.5 Hz, 1H), 8.24 (s, 1H), 7.99–7.92 (m, 2H), 7.61–7.57 (m, 2H), 5.15–5.04 (m, 1H), 2.56 (t, J = 6.0 Hz, 2H), 2.22–2.08 (m, 2H), 1.92–1.84 (m, 1H), 1.82–1.63 (m, 3H), 1.05 (t, J = 7.6 Hz, 3H). ^{13}C NMR (150 MHz, DMSO-d_6): δ = 172.9, 150.3, 147.4, 144.0, 142.7, 135.2, 134.3, 132.9, 130.8, 119.2, 111.1, 44.7, 29.4, 29.0, 27.2, 19.5, 10.5. HRMS ($C_{19}H_{19}N_3O$): calcd 305.1528; found 305.1534.

Enantiomer (−)-(S)-6. LC–MS: t_R = 1.21 min, 99% (265 nm); t_R = 1.21 min, 99% (225 nm). ^{1}H NMR (600 MHz, DMSO-d_6): δ = 8.39 (s, 1H), 8.28 (d, J = 8.5 Hz, 1H), 8.24 (s, 1H), 7.99–7.92 (m, 2H), 7.61–7.57 (m, 2H), 5.15–5.04 (m, 1H), 2.56 (t, J = 6.0 Hz, 2H), 2.22–2.08 (m, 2H), 1.92–1.84 (m, 1H), 1.82–1.63 (m, 3H), 1.05 (t, J = 7.6 Hz, 3H). ^{13}C NMR (150 MHz, DMSO-d_6): δ = 172.9, 150.3, 147.4, 144.0, 142.7, 135.2, 134.3, 132.9, 130.8, 119.2, 111.1, 44.7, 29.4, 29.0, 27.2, 19.5, 10.5. HRMS ($C_{19}H_{19}N_3O$): calcd 305.1528; found 305.1527.

Preparation of (+)-(R)-6 from Enantiopure Benzonitrile (+)-(R)-4. (+)-(R)-N-(4-(4-Cyanophenyl)-5,6,7,8-tetrahydroisoquinolin-8-yl)propionamide ((+)-(R)-6). To a stirred solution of (+)-(R)-4-[(8R)-8-amino-5,6,7,8-tetrahydroisoquinolin-4-yl]benzonitrile ((+)-(R)-4, 71 mg, 285 μmol) and propionic acid (23.4 μL, 313 μmol) in CH_2Cl_2 (1.5 mL) at 0 °C under argon was added EDCI (60.1 mg, 313 μmol). Stirring was continued overnight and the reaction mixture was allowed to warm to rt. The reaction mixture was poured into aqueous 10% KH_2PO_4 solution followed by extraction with EtOAc (3×). The organic phases were washed once with aqueous 10% KH_2PO_4, aqueous saturated $NaHCO_3$, and aqueous saturated NaCl solution. The organic phase was dried over Na_2SO_4, filtered, and evaporated to afford after precipitation (CH_2Cl_2/n-pentane) the title compound (70 mg, 81%) as light brown solid. The analytical characterization data obtained are identical to the data for (+)-(R)-6 derived from chiral separation of (rac)-6.

Preparation of (rac)-N-(4-(4-Cyanophenyl)-5,6,7,8-tetrahydroisoquinolin-8-yl)isobutyramide (7). A solution of (rac)-4-(8-amino-5,6,7,8-tetrahydroisoquinolin-4-yl)benzonitrile (4, 62.3 mg, 250 μmol) in CH_2Cl_2 (3.6 mL) cooled to −20 °C was treated with isobutyryl chloride (32.1 μL, 300 μmol) and triethylamine (69.7 μL, 500 μmol). After 30 min, an additional drop of isobutyryl chloride was added, and after 5 min the mixture was treated with MeOH (0.2 mL) and extracted with water/EtOAc (3×). The organic phases were dried over Na_2SO_4, filtered, and evaporated under reduced pressure. Purification by flash chromatography [20 g SiO_2, Telos cartridge, CH_2Cl_2/MeOH (1% → 2%)] and precipitation from CH_2Cl_2 with n-pentane gave the title compound (50 mg, 63%) as an off-white powder. LC–MS: t_R = 1.60 min, 100% (265 nm); t_R = 1.60 min, 99% (225 nm). ^{1}H NMR (300 MHz, DMSO-d_6): δ = 8.36 (s, 1H), 8.25 (d, J = 8.3 Hz, 1H), 8.24 (s, 1H), 7.95 (d, J = 8.3 Hz, 2H), 7.59 (d, J = 8.5 Hz, 2H), 5.08 (ddd, J = 6.1 Hz, 1H), 2.60–2.53 (m, 2H), 2.42 (dq, J = 6.9 Hz, 1H), 1.96–1.83 (m, 1H), 1.84–1.60 (m, 3H), 1.07 (d, J = 6.9 Hz, 3H), 1.04 (d, J = 6.9 Hz, 3H). ^{13}C NMR (150 MHz, DMSO-d_6): δ = 175.7, 149.7, 147.0, 143.6, 142.2, 134.8, 133.9, 132.4, 130.3, 118.7, 110.6, 44.2, 33.9, 28.9, 26.8, 19.7, 19.5, 19.1. HRMS ($C_{20}H_{21}N_3O$): calcd 319.1685; found 319.1685.

Preparation of (rac)-N-(4-(3,4-Difluorophenyl)-5,6,7,8-tetrahydroisoquinolin-8-yl)propionamide (8). (rac)-N-(4-Bromo-5,6,7,8-tetrahydroisoquinolin-8-yl)propionamide (17, 60 mg, 212 μmol) and 3,4-difluorophenylboronic acid (40.2 mg, 254 μmol) were dissolved in ethanol (3.8 mL) to give a light brown solution. Na_2CO_3 (24.7 mg, 233 μmol) dissolved in water (0.6 mL) was added followed by tetrakis(triphenylphosphine)palladium (0) (7.4 mg, 6.4 μmol) after evacuation and replacing with argon (cycle repeated 5×). The solution was then heated at 85 °C overnight. The reaction was treated with an aqueous 10% NaCl solution and extracted with EtOAc (3×). The organic phases were washed again with an aqueous 10% NaCl solution, dried over Na_2SO_4, filtered, and evaporated under reduced pressure to give a brown foam which was purified by flash chromatography [20 g SiO_2, Telos cartridge, CH_2Cl_2/isopropanol (3% → 5%)]. Precipitation from CH_2Cl_2 with n-pentane gave the final compound (57 mg, 85%) as a light brown foam. LC–MS: t_R = 1.50 min, 98% (265 nm); t_R = 1.50 min, 97% (225 nm). ^{1}H NMR (600 MHz, DMSO-d_6): δ = 8.36 (s, 1H), 8.27 (d, J = 8.5 Hz, 1H), 8.23 (s, 1H), 7.56–7.52 (m, 1H), 7.52–7.49 (m, 1H), 7.23–7.20 (m, 1H), 5.11–5.07 (m, 1H), 2.58 (t, J = 6.1 Hz, 2H), 2.18–2.12 (m, 2H), 1.90–1.85 (m, 1H), 1.81–1.75 (m, 1H), 1.74–1.68 (m, 1H), 1.72–1.66 (m, 1H), 1.05 (t, J = 7.6 Hz, 3H). ^{13}C NMR (150 MHz, DMSO-d_6): δ = 172.5, 149.5, 149.3 (m), 149.2 (m), 147.2, 143.8, 134.6 (m), 134,3, 133.8, 126.4 (dd, J_{CF} = 6.3, 3.2 Hz), 118.5 (d, J_{CF} = 17.4 Hz), 117.6 (d, J_{CF} = 17.0 Hz), 44.2, 28.9, 28.5, 26.7, 19.1, 10.0. HRMS ($C_{18}H_{18}F_2N_2O$): calcd 316.1387; found 316.1387.

Preparation of (rac)-N-(4-(2,4,5-Trifluorophenyl)-5,6,7,8-tetrahydroisoquinolin-8-yl)propionamide (9). (rac)-N-(4-

Bromo-5,6,7,8-tetrahydroisoquinolin-8-yl)propionamide (**17**, 105 mg, 370 μmol) and 2,4,5-trifluorophenylboronic acid (78.1 mg, 444 μmol) were dissolved in ethanol (6.7 mL) to give a light brown solution. Na_2CO_3 (43.1 mg, 407 μmol) dissolved in water (1.1 mL) was added followed by tetrakis(triphenylphosphine)palladium (0) (12.8 mg, 11 μmol) after evacuation and replacing with argon (cycle repeated 5×). The solution was then heated at 85 °C overnight. The reaction was treated with an aqueous 10% NaCl solution and extracted with EtOAc (3×). The organic phases were washed again with an aqueous 10% NaCl solution, dried over Na_2SO_4, filtered, and evaporated under reduced pressure to give a brown foam which was purified by flash chromatography [20 g SiO_2, Telos cartridge, CH_2Cl_2/isopropanol (3% → 5%)]. Precipitation from CH_2Cl_2 with *n*-pentane gave the final compound (49 mg, 40%) as a white foam. LC−MS: t_R = 1.73 min, 98% (265 nm); t_R = 1.73 min, 96% (225 nm). ^{1}H NMR (600 MHz, DMSO-d_6): δ = 8.40 (s, 1H), 8.36−8.26 (m, 1H), 8.24 (s, 1H), 7.75−7.70 (m, 1H), 7.58 (br s, 1H), 5.09 (q, *J* = 6.9 Hz, 1H), 2.46 (br d, *J* = 6.2 Hz, 2H), 2.19−2.13 (m, 2H), 1.91−1.86 (m, 1H), 1.82−1.77 (m, 1H), 1.72−1.67 (m, 2H), 1.06 (t, *J* = 7.6 Hz, 3H). ^{13}C NMR (150 MHz, DMSO-d_6): δ = 172.5, 154.6 (dd, J_{CF} = 243.0, 9.8 Hz), 150.0, 147.7, 147.7 (m), 146.0 (m), 144.7, 133.9, 128.6, 121.3 (m), 119.6 (m), 106.4 (dd, J_{CF} = 29.2, 21.1 Hz), 44.2, 29.0, 28.5, 26.1, 19.0, 10.0. HRMS ($C_{18}H_{17}F_3N_2O$): calcd 334.1293; found 334.1294.

Preparation of (*rac*)-*N*-(4-(4-Chloro-2-fluorophenyl)-5,6,7,8-tetrahydroisoquinolin-8-yl)propionamide (10). (*rac*)-*N*-(4-Bromo-5,6,7,8-tetrahydroisoquinolin-8-yl)propionamide (**17**, 116 mg, 565 μmol) and 4-chloro-2-fluorophenylboronic acid (122 mg, 678 μmol) were dissolved in ethanol (10.2 mL) to give a light brown solution. Na_2CO_3 (65.9 mg, 622 μmol) dissolved in water (1.7 mL) was added followed by tetrakis(triphenylphosphine)palladium(0) (19.6 mg, 17 μmol) after evacuation and replacing with argon (cycle repeated 5×). The solution was then heated at 85 °C overnight. The reaction was treated with an aqueous 10% NaCl solution and extracted with EtOAc (3×). The organic phases were washed again with an aqueous 10% NaCl solution, dried over Na_2SO_4, filtered, and evaporated under reduced pressure to give a brown foam which was purified by flash chromatography [50 g SiO_2, Telos cartridge, CH_2Cl_2/isopropanol (3% → 6%)]. Precipitation from CH_2Cl_2 with *n*-pentane gave the final compound (132 mg, 70%) as an off-white foam. LC−MS: t_R = 2.19 min, 93% (265 nm); t_R = 2.11 min, 99% (220 nm). ^{1}H NMR (600 MHz, DMSO-d_6): δ = 8.39 (s, 1H), 8.35−8.25 (m, 1H), 8.23 (s, 1H), 7.60 (dd, *J* = 9.8, 1.9 Hz, 1H), 7.43−7.40 (m, 1H), 7.40 (br d, *J* = 7.9 Hz, 1H), 5.12−5.08 (m, 1H), 2.46−2.41 (m, 2H), 2.19−2.13 (m, 2H), 1.91−1.85 (m, 1H), 1.82−1.76 (m, 1H), 1.69 (br t, *J* = 7.0 Hz, 1H), 1.71−1.66 (m, 1H), 1.05 (t, *J* = 7.6 Hz, 3H). ^{13}C NMR (150 MHz, DMSO-d_6): δ = 172.5, 159.2 (d, J_{CF} = 247.9 Hz), 149.9, 147.5, 144.7, 133.9 (d, J_{CF} = 10.5 Hz), 133.8, 132.9, 129.5, 125.1 (d, J_{CF} = 3.3 Hz), 123.6 (d, J_{CF} = 16.8 Hz), 116.4 (d, J_{CF} = 26.1 Hz), 44.2, 29.0, 28.5, 26.2, 18.9, 10.0. HRMS ($C_{18}H_{18}ClFN_2O$): calcd 332.1091; found 332.10949.

Preparation of (*rac*)-*N*-(4-(4-Chloro-3-fluorophenyl)-5,6,7,8-tetrahydroisoquinolin-8-yl)propionamide (11). (*rac*)-*N*-(4-Bromo-5,6,7,8-tetrahydroisoquinolin-8-yl)propionamide (**17**, 116 mg, 565 μmol) and 4-chloro-3-fluorophenylboronic acid (84.9 mg, 300 μmol) were dissolved in ethanol (5.4 mL) to give a light brown solution. Na_2CO_3 (35.0 mg, 330 μmol) dissolved in water (1.0 mL) was added followed by tetrakis(triphenylphosphine)palladium (0) (10.4 mg, 9 μmol) after evacuation and replacing with argon (cycle repeated 5×). The solution was then heated at 85 °C overnight. The reaction was treated with an aqueous 10% NaCl solution and extracted with EtOAc (3×). The organic phases were washed again with an aqueous 10% NaCl solution, dried over Na_2SO_4, filtered, and evaporated under reduced pressure to give a brown foam which was purified by flash chromatography [20 g SiO_2, Telos cartridge, CH_2Cl_2/isopropanol (3% → 5%)]. Precipitation from CH_2Cl_2 with *n*-pentane gave the final compound (83 mg, 83%) as a light brown foam. LC−MS: t_R = 2.11 min, 98% (265 nm); t_R = 2.11 min, 99% (220 nm). ^{1}H NMR (300 MHz, DMSO-d_6): δ = 8.37 (s, 1H), 8.27 (d, *J* = 8.3 Hz, 1H), 8.24 (s, 1H), 7.69 (dd, *J* = 8.1 Hz, 1H), 7.49 (dd, *J* = 10.3, 1.8 Hz, 1H), 7.24 (dd, *J* = 8.3, 1.4 Hz, 1H), 5.09 (ddd, *J* = 7.3 Hz, 1H),

2.64−2.55 (m, 2H), 2.15 (qd, *J* = 7.6, 2.6 Hz, 2H), 1.95−1.63 (m, 4H), 1.05 (t, *J* = 7.6 Hz, 3H). ^{13}C NMR (150 MHz, DMSO-d_6): δ = 172.9, 157.5 (d, J_{CF} = 247.3 Hz), 150.0, 147.5, 144.3, 138.8 (d, J_{CF} = 7.4 Hz), 134.6, 134.3, 131.1, 127.2 (d, J_{CF} = 3.3 Hz), 119.5 (d, J_{CF} = 17.3 Hz), 118.3 (d, J_{CF} = 3.3 Hz), 44.7, 29.4, 29.0, 27.2, 19.5, 10.5. HRMS ($C_{18}H_{18}ClFN_2O$): calcd 332.1092; found 332.1101.

Experimental Details for Protein Crystallization and Structure Determination of CYP11B2 with Compound 11. CYP11B2 protein was overexpressed in *E. coli* and purified with nickel affinity and ion exchange chromatography. The ligand complex was cocrystallized by vapor diffusion in sitting drops with 10% PEG3350 in 90 mM ammonium citrate (pH 7.0). Thin plates grew after several days and were flash-frozen after addition of 20% ethylene glycol. X-ray diffraction images were collected at 100 K at the beamline X10SA (PXII) of the Swiss Light Source (SLS) using a Pilatus pixel detector.

In Vitro Assay for the Determination of CYP11B2 and CYP11B1 Inhibition. CYP11B1 and CYP11B2 proteins were expressed in a human renal leiomyoblastoma cell line (ATCC number CRL-1440). qPCR revealed that these cells express FDXR and FDX, two proteins that are crucial for the enzymatic activity of CYP11B enzymes and importantly do not express detectable levels of CYP11B1 or CYP11B2 activity. The cells are grown in ATCC-formulated McCoy's 5a medium modified (catalog no. 30-2007) containing 10% fetal bovine serum. Stable cells expressing ectopically CYP11B1 or CYP11B2 from human, cynomolgus monkey, or mouse were developed by transfecting appropriate expression plasmids. The plasmids contain the cDNA (GeneCopoeia) for either CYP11B1 or CYP11B2 from the appropriate species (mouse, cynomolgus monkey, or man) under the control of a CMV promoter and the neomycin resistance marker. Using electroporation expression plasmid were transfected into cells, and these cells were then selected for expressing the given resistance markers. Individual cell clones are then selected (400 μg mL$^{−1}$ G-418; Geneticin) and assessed for displaying the desired enzymatic activity using 11-deoxycorticosterone (CYP11B2) or 11-deoxycortisol (CYP11B1) as a substrate. Cellular enzyme assays were performed in DMEM/F12 medium containing 2.5% charcoal treated FCS and appropriate concentration of substrate (1 μM 11-deoxycorticosterone or 11-deoxycortisol). For assaying enzymatic activity, cells were plated onto 96-well plates and incubated for 16 h. An aliquot of the supernatant was then transferred and analyzed for the concentration of the expected product (aldosterone for CYP11B2; cortisol for CYP11B1). The concentrations of these steroids can be determined using HTRF (homogeneous time-resolved fluorescence) assays from CisBio analyzing either aldosterone or cortisol. Inhibition of the release of produced steroids can be used as a measure of the respective enzyme inhibition by test compounds added during the cellular enzyme assay. The dose dependent inhibition of enzymatic activity by a compound is calculated by means of plotting added inhibitor concentrations (*x*-axes) vs measured steroid/product level (*y*-axes). The inhibition is then calculated by fitting the following four-parameter sigmoidal function [Morgan−Mercer−Flodin (MMF) model] to the raw data points using the least-squares method:

$$y = \frac{AB + Cx^D}{B + x^D}$$

where *A* is the maximum *y* value, *B* is the EC_{50} value determined using XLfit, *C* is the minimum *y* value, and *D* is the slope value. The maximum value *A* corresponds to the amount of steroid produced in the absence of an inhibitor, and the value *C* corresponds to the amount of steroid detected when the enzyme is fully inhibited.

Experimental Details for in Vivo db/db Mouse Experiments. Male db/db mice (5 weeks old) were ordered from Taconic Biosciences (Hudson, NY, USA) and were housed in groups to acclimate to the Roche facility. The animals were kept on a 12 h light/dark cycle and were fed with NIH no. 31M rodent diet (Harlan Laboratories, Indianapolis, IN, USA) with access to tap water ad libitum. Right before the age of 12 weeks, mice were randomized according to body weight and blood glucose (fed conditions), measured with Alphatrak glucometer (Abbott Laboratories, Chicago, IL, USA). Treatments were prepared as food admix by SSniff (Soest,

Germany) in NIH no. 31M rodent diet and were given for 3 weeks. At the end of the treatment, animals were sacrificed by decapitation after isoflurane (Forène, Abbott Laboratories, Chicago, IL, USA) anesthesia, and blood was sampled on EDTA-coated tubes (Microvette 500 K3E, Sarstedt, Nümbrecht, Germany) for steroid level determinations. Blood was centrifuged at 10 000 rpm for 15 min at 4 °C, and plasma was sampled and steroid levels were measured by LC–MS–MS methodology (see Supporting Information).

Experimental Details for in Vivo Cynomolgus Monkey Experiments. Non-naive grouped male cynomolgus monkeys (*Macaca fascicularis*) were kept in cages on a 12 h light–dark cycle with natural light in 50–60% humidity and 22.5–22.8 °C. Animals received the diet 3448 EM S12 (80 g 7 kg^{-1} day^{-1} animal^{-1}; Provimi-Kliba, Kaiseraugst, Switzerland) 2–3 times daily, on top of daily fruits, vegetables, and nuts. Water access was ad libitum. Animals identified as good Synacthen (Novartis, Basel, Switzerland) responders participated in the study under the following conditions: at least a 2-fold increase of plasma aldosterone, cortisol, and corticosterone production should be measured 1 h after intramuscular acute application of Synacthen. On the day of the experiment, the monkeys were moved from their group cages and individually housed in stainless-steel mesh cages (*H* 1.5 m × *L* 1.2 m × *W* 0.8 m) according to the Swiss regulation on animal welfare. For oral gavage (po) all samples were analyzed using routine protein precipitation technique followed by LC–MS–MS analysis. PK parameters were calculated using noncompartmental analysis (Table S1). Oral treatment and Synacthen were given as follows: *T* = 0, oral dosing of 2 monkeys per group (vehicle or compound (+)-(*R*)-**6**) with compound administered as suspension in hydroxyethylcellulose, polysorbate 80, methyparaben, and propylparaben vehicle using 2 mL kg^{-1} administration volume; *T* = +5 min, intramuscular application of 14.5 μg kg^{-1} Synacthen. Blood samples were collected 15 min, 30 min, 1 h, 2 h, 4 h, and 6 h after compound or vehicle application. At each time point, 1.2 mL blood was collected in EDTA-coated tubes (BD Vacutainer K2 EDTA, Becton Dickinson, Franklin Lakes, NJ, USA) for plasma mineral corticoids and compound concentration measurements. Blood was centrifuged at 10 000 rpm for 15 min at 4 °C. Subsequently, plasma was separated and stored at −20 °C for further analysis. Plasma steroids, % inhibition of CYP11B1 and CYP11B2, and exposure data for (+)-(*R*)-**6** were analyzed from all time points by LC–MS–MS methodology (see Supporting Information).

Animals in Research. Animal work was performed according to the Swiss federal law for animal protection and was approved by the Veterinary Office Basel. Animals were provided an acclimation period of >5 days before use, conventional hygienic conditions for housing (temperature of 20–24 °C, minimum relative humidity of 40%, light/dark cycle of 12 h), and standard diet; access to food and drinking water was ad libitum. Specific details on permissions can be provided upon request.

ASSOCIATED CONTENT

Ⓢ Supporting Information

The Supporting Information is available free of charge on the ACS Publications website at DOI: 10.1021/acs.jmedchem.5b00851.

Details on the acute effects of LCI699 (**2**) on steroid levels in db/db mice; calculation of CYP11B2 and CYP11B1 enzyme inhibition levels in cynomolgus monkey and pharmacokinetics for (+)-(*R*)-**6**; method for the multiplex determination of a CYP11B1/B2 related seven steroid panel in cynomolgus monkey plasma by LC–MS–MS; X-ray crystallographic analysis of bromo tetrahydroisoquinoline intermediate (−)-(*S*)-**16** (PDF)

Molecular formula strings (XLSX)

Accession Codes

Atomic coordinates of compound **11** have been deposited in the Protein Data Bank with accession number 4ZGX.

AUTHOR INFORMATION

Corresponding Authors
*J.D.A.: phone, 0041 61 6887738; fax, 0041 61 6886459; e-mail,: johannes.aebi@roche.com.
*K.A.: phone, 0041 61 6889587; e-mail, kurt.amrein@roche.com.
*A.V.M.: phone, 0041 61 6871384; e-mail, alexander_v.mayweg@roche.com.

Author Contributions
All authors have given approval to the final version of the manuscript.

Notes
The authors declare no competing financial interest.

ABBREVIATIONS USED

AcOH, acetic acid; *n*-BuLi, *n*-butyllithium; CYP, cytochrome P450 enzyme; DMAP, 4-dimethylaminopyridine; EDCI, *N*-(3-dimethylaminopropyl)-*N*′-ethylcarbodiimide hydrochloride; EtOAc, ethyl acetate; EtOH, ethanol; MeOH, methanol; PA, primary aldosteronism; rt, room temperature; SF, selectivity factor

REFERENCES

(1) Hoogwerf, B. J. Renin-angiotensin system blockade and cardiovascular and renal protection. *Am. J. Cardiol.* **2010**, *105* (suppl), 30A–35A.

(2) Alderman, M. H.; Madhavan, S.; Ooi, W. L.; Cohen, H.; Sealey, J. E.; Laragh, J. H. Association of the renin-sodium profile with the risk of myocardial infarction in patients with hypertension. *N. Engl. J. Med.* **1991**, *324*, 1098–1104.

(3) Leoncini, G.; Viazzi, F.; Pontremoli, R. RAAS inhibition and renal protection. *Curr. Pharm. Des.* **2012**, *18*, 971–980.

(4) Zannad, F.; McMurray, J. J.; Krum, H.; van Veldhuisen, D. J.; Swedberg, K.; Shi, H.; Vincent, J.; Pocock, S. J.; Pitt, B. Eplerenone in patients with systolic heart failure and mild symptoms. *N. Engl. J. Med.* **2011**, *364*, 11–21.

(5) Pitt, B.; Remme, W.; Zannad, F.; Neaton, J.; Martinez, F.; Roniker, B.; Bittman, R.; Hurley, S.; Kleiman, J.; Gatlin, M. Eplerenone, a selective aldosterone blocker, in patients with left ventricular dysfunction after myocardial infarction. *N. Engl. J. Med.* **2003**, *348*, 1309−1321.

(6) Pitt, B.; Zannad, F.; Remme, W. J.; Cody, R.; Castaigne, A.; Perez, A.; Palensky, J.; Wittes, J. The effect of spironolactone on morbidity and mortality in patients with severe heart failure. Randomized aldactone evaluation study investigators. *N. Engl. J. Med.* **1999**, *341*, 709−717.

(7) Williams, G. H. Essential hypertension as an endocrine disease. *Endocrinol. Metab. Clin. N. Am.* **1994**, *23*, 429−444.

(8) Hu, Q.; Yin, L.; Hartmann, R. W. Aldosterone synthase inhibitors as promising treatments for mineralocorticoid dependent cardiovascular and renal diseases. *J. Med. Chem.* **2014**, *57*, 5011−5022.

(9) Azizi, M.; Amar, L.; Ménard, J. Aldosterone synthase inhibition in humans. *Nephrol., Dial., Transplant.* **2013**, *28*, 36−43.

(10) Bassett, M. H.; White, P. C.; Rainey, W. E. The regulation of aldosterone synthase expression. *Mol. Cell. Endocrinol.* **2004**, *217*, 67−74.

(11) Cerny, M. A. Progress towards clinically useful aldosterone synthase inhibitors. *Curr. Top. Med. Chem.* **2013**, *13*, 1385−1401.

(12) Lea, W. B.; Kwak, E. S.; Luther, J. M.; Fowler, S. M.; Wang, Z.; Ma, J.; Fogo, A. B.; Brown, N. J. Aldosterone antagonism or synthase inhibition reduces end-organ damage induced by treatment with angiotensin and high salt. *Kidney Int.* **2009**, *75*, 936−944.

(13) Fiebeler, A.; Nussberger, J.; Shagdarsuren, E.; Rong, S.; Hilfenhaus, G.; Al-Saadi, N.; Dechend, R.; Wellner, M.; Meiners, S.; Maser-Gluth, C.; Jeng, A. Y.; Webb, R. L.; Luft, F. C.; Muller, D. N. Aldosterone synthase inhibitor ameliorates angiotensin II-induced organ damage. *Circulation* **2005**, *111*, 3087−3094.

(14) Amar, L.; Azizi, M.; Ménard, J.; Peyrard, S.; Watson, C.; Plouin, P.-F. Aldosterone synthase inhibition with LCI699: A proof-of-concept study in patients with primary aldosteronism. *Hypertension* **2010**, *56*, 831−838.

(15) Ménard, J.; Rigel, D. F.; Watson, C.; Jeng, A. Y.; Fu, F.; Beil, M.; Liu, J.; Chen, W.; Hu, C.-W.; Leung-Chu, J.; LaSala, D.; Liang, G.; Rebello, S.; Zhang, Y.; Dole, W. P. Aldosterone synthase inhibition: cardiorenal protection in animal disease models and translation of hormonal effects to human subjects. *J. Transl. Med.* **2014**, *12*, 340/1−340/43.

(16) Ries, C.; Lucas, S.; Heim, R.; Birk, B.; Hartmann, R. W. Selective aldosterone synthase inhibitors reduce aldosterone formation *in vitro* and *in vivo*. *J. Steroid Biochem. Mol. Biol.* **2009**, *116*, 121−126.

(17) CCDC 1415366 contains the supplementary crystallographic data for this paper. These data can be obtained free of charge from The Cambridge Crystallographic Data Centre via www.ccdc.cam.ac.uk/data_request/cif.

(18) Sequence alignment and homology model building were performed with the MOE software package using the crystal structure of bovine CYP11A1 (PDB code 3MZS) as template. *Molecular Operating Environment* (MOE), version 2011; Chemical Computing Group: Quebec, Canada See the following: Mast, N.; Annalora, A. J.; Lodowski, D. T.; Palczewski, K.; Stout, C. D.; Pikuleva, I. A. Structural basis for three-step sequential catalysis by the cholesterol side chain cleavage enzyme CYP11A1. *J. Biol. Chem.* **2011**, *286*, 5607−5613. Sequence identity of CYP11A1 with CYP11B1 and CYP11B2 is 37%. The heme cofactor and the bound ligand 22-hydroxycholesterol from 3MZS were kept during model building, and the best scoring minimized homology model was selected. This was further refined by subsequent relaxation of the binding site using Moloc. See the following: Gerber, P. R.; Müller, K. MAB, a generally applicable molecular force field for structure modelling in medicinal chemistry. *J. Comput.-Aided Mol. Des.* **1995**, *9*, 251−268.

(19) The log *D* values were measured spectrophotometrically at pH 7.4 in an 1-octanol/50 mM TAPSO buffer system containing 5% (v/v) DMSO.

(20) Aqueous solubility was measured from lyophilized DMSO stock solutions spectrophotometrically at pH 6.5 in a 50 mM phosphate buffer (lyophilization solubility assay, Lysa).

(21) Pampa (parallel artificial membrane permeation assay): low, Pe < 0.1; medium, 0.1 < Pe < 1.0; high, Pe > 1.0. See the following: Kansy, M.; Senner, F.; Gubernator, K. *J. Med. Chem.* **1998**, *41*, 1007−1010.

(22) Strushkevich, N.; Gilep, A. A.; Shen, L.; Arrowsmith, C. H.; Edwards, A. M.; Usanov, S. A.; Park, H.-W. Structural insights into aldosterone synthase substrate specificity and targeted inhibition. *Mol. Endocrinol.* **2013**, *27*, 315−324.

(23) Briones, A. M.; Nguyen Dinh Cat, A.; Callera, G. E.; Yogi, A.; Burger, D.; He, Y.; Corrêa, J. W.; Gagnon, A. M.; Gomez-Sanchez, C. E.; Gomez-Sanchez, E. P.; Sorisky, A.; Ooi, T. C.; Ruzicka, M.; Burns, K. D.; Touyz, R. M. Adipocytes produce aldosterone through calcineurin-dependent signaling pathways - implications in diabetes mellitus-associated obesity and vascular dysfunction. *Hypertension* **2012**, *59*, 1069−1078.

(24) Coleman, D. L.; Burkart, D. L. Plasma corticosterone concentrations in diabetic (*db*) mice. *Diabetologia* **1977**, *13*, 25−26.

(25) Manuscript in preparation.

(26) Hoyt, S. B.; Park, M. K.; London, C.; Xiong, Y.; Tata, J.; Bennett, D. J.; Cooke, A.; Cai, J.; Carswell, E.; Robinson, J.; et al. Discovery of benzimidazole CYP11B2 inhibitors with *in vivo* activity in rhesus monkeys. *ACS Med. Chem. Lett.* **2015**, *6*, 573−578.